electronics

Article

Redesign of Channel Codes for Joint Source-Channel Coding Systems over One-Dimensional Inter-Symbol-Interference Magnetic Recording Channels

Ying Sun, Chen Chen *, Sanya Liu, Qiwang Chen and Lin Zhou

School of Information Science and Engineering, Huaqiao University, Xiamen 361021, China
* Correspondence: chen_chen@hqu.edu.cn

Abstract: Although the joint source-channel coding (JSCC) system based on double protograph low-density parity-check (DP-LDPC) codes has been shown to possess excellent error performance over additive white Gaussian noise (AWGN) channels, it cannot perform well over one-dimensional inter-symbol-interference (OD-ISI) magnetic recording channels. In this study, a new JSCC system with a three-stage serially concatenated framework of Turbo equalization is firstly proposed for OD-ISI magnetic recording channels. Then, a modified joint protograph extrinsic information transfer (M-JPEXIT) algorithm is put forward to analyze the convergence-performance of the proposed system. By applying the M-JPEXIT algorithm, the channel codes are redesigned for this system to improve the error performance. Both the M-JPEXIT analysis and the bit-error-rate (BER) simulation results show the performance improvement of the proposed channel codes, especially in the water-fall region.

Keywords: JSCC; OD-ISI magnetic recording channels; M-JPEXIT; redesign

Citation: Sun, Y.; Chen, C.; Liu, S.; Chen, Q.; Zhou, L. Redesign of Channel Codes for Joint Source-Channel Coding Systems over One-Dimensional Inter-Symbol-Interference Magnetic Recording Channels. *Electronics* **2022**, *11*, 3490. https://doi.org/10.3390/electronics11213490

Academic Editor: Luis Castedo

Received: 25 August 2022
Accepted: 22 October 2022
Published: 27 October 2022

1. Introduction

Joint source-channel coding (JSCC) can achieve significant coding gain improvement compared with the traditional separate coding in finite block-length transmission [1,2]. Among different JSCC schemes, low-density parity-check (LDPC) codes [3] were shown to be good candidates for both source and channel codes because of their outstanding error-correction performance [4]. Owing to the properties of fast encoding structure and high decoding speed, protograph LDPC (PLDPC) codes [5] were further introduced into JSCC systems, named as double protograph LDPC (DP-LDPC) systems [6]. Moreover, substantial efforts have been invested in improving the water-fall region and error-floor of the DP-LDPC system over additive white Gaussian noise (AWGN) channels [7–14]. For instance, a redesigning scheme for channel codes in the DP-LDPC system was put forward in [7]. A joint optimization procedure for source and channel code pairs was proposed in [9]. The optimization of the DP-LDPC system through joint design of the source code, the channel code, the type-1 connection edge and the type-2 connection edge was addressed in [11], and a design criteria was presented for connections between variable nodes (VNs) of the source protograph and check node (CNs) of the channel protograph in [12], which results in a lower error floor. Nonetheless, the most optimization schemes for the codes in the DP-LDPC system are based on AWGN channels, the designs of counterparts over memory channels are relatively unexplored.

For the magnetic recording (MR) channel with inter-symbol-interference (ISI) memory, ISI is an important factor that deteriorates the reliability of stored data over MR channels. Several coding schemes have been developed to enhance the reliability of MR channels. For instance, to alleviate the effect of the ISI , Turbo equalization [15,16] is extensively utilized in such channels. The main idea of Turbo equalization is to treat the ISI channel and the error correction code (ECC) as the inner code and the outer code of a serial concatenated scheme, respectively. As an outstanding ECC, LDPC code has been applied as the outer

code in MR channels [17,18]. The optimization schemes of the channel coding and decoding have been proposed in [19–21] for ISI channels. A novel alternating direction method of multipliers-based decoding method has been derived for LDPC codes over ISI channels in [20], and a novel channel coding autoencoder has been presented for AWGN channels with discrete-time ISI effects in [21]. Moreover, many researchers have endeavored to design good PLDPC codes over one-dimensional inter-symbol-interference (OD-ISI) MR channels and two-dimensional inter-symbol-interference (TD-ISI) MR channels [22–28]. For example, a new design scheme and three new types of PLDPC codes were proposed for the partial response (PR) channel model in [22]. The design of PLDPC codes which can approach the independent and uniformly distributed (i.u.d.) capacity of PR channels was addressed in [24]. Moreover, a family of rate-compatible PLDPC codes approaching the i.u.d. capacity of ISI channels was produced in [25]. For the TD-ISI MR channel, the design of PLDPC codes and non-binary PLDPC codes were presented in [26,27]. In particularly, a survey-type of paper [28] provided an introduction to the latest research advancements in PLDPC-code design over MR channels. However, the above-mentioned works for MR channels both aimed at designing channel codes based on separate coding structures, rather than JSCC systems. Considering that the redundancy left by the source encoder can be exploited at the joint source-channel decoder (JSCD) to reduce the bit-error-rate (BER) over AWGN channels, the JSCC system over MR channels also need to be investigated. As is shown in [7], the optimal channel code in separate systems is no longer optimal in joint systems. Therefore, the design for channel codes in the JSCC system over MR channels should be looked into as well.

With this motivation, this work mainly investigates the DP-LDPC system over OD-ISI MR channels and proposes a re-design scheme for channel codes of this system. To be more specific, firstly, a three-stage serially concatenated framework of Turbo equalization is proposed in this system. Moreover, to analyze the convergence-performance of the proposed system, the modified joint protograph extrinsic information transfer (M-JPEXIT) algorithm is designed to investigate the mutual information (MI) evolution among the three components. Additionally, by means of the M-JPEXIT algorithm, a re-design scheme for channel codes is put forward to improve the error performance. Both the M-JPEXIT analysis and the BER simulation results indicate the performance improvement of the re-design scheme in the water-fall region. The main contributions of this paper are as follows.

(1) To exploit the redundancy left by the source encoder, a new JSCC system with a three-stage serially concatenated framework of Turbo equalization is proposed for OD-ISI MR channels.
(2) In order to analyze the asymptotic-performance for the proposed system, a M-JPEXIT algorithm is designed, which investigates the MI evolution among the Bahl–Cocke–Jelinek–Raviv (BCJR) detector, the channel decoder and the source decoder.
(3) An optimization algorithm for channel codes is put forward to improve the error performance of the proposed system by means of the M-JPEXIT algorithm, which takes both degree-1 VN and the type-1 connection edge into consideration.

In summary, this work concentrates on the design of the DP-LDPC system over OD-ISI MR channels and improving the error performance of this system, which can enrich the analysis of JSCC systems over memory channels.

The organization of this paper is as follows. Section 2 presents the system model. Section 3 proposes the M-JPEXIT algorithm for this system and a re-design scheme for channel codes of this system is also presented. Section 4 presents and discusses the simulation results. Section 5 concludes the paper.

2. System Model

The system model is described in Figure 1b. At the transmitter, we consider a binary independent and identically distributed (i.i.d.) Bernoulli (p) source sequence $\mathbf{s}$ with entropy

$$H = -p\log_2 p - (1-p)\log_2(1-p), \tag{1}$$

where $p < 1/2$. The source is first compressed by an un-punctured PLDPC code and then encoded by another punctured PLDPC code. The encoded sequence is binary-phase-shift-keying (BPSK) modulated into $\mathbf{x} = (x_1, x_2, \ldots, x_m)$, where m is the length of modulated symbol sequence. The OD-ISI MR channel can be modeled as a discrete channel with ISI memory. For transmission over a OD-ISI MR channel, the output of the channel $\mathbf{y} = (y_1, y_2, \ldots, y_m)$ can be expressed as a PR polynomial plus a Gaussian noise, which is given by

$$y_i = \sum_{j=0}^{k} h_j x_{i-j} + n_i, \tag{2}$$

where $i = 1, 2, \ldots, m$, k is the length of the channel memory, $h_j (j = 0, 1, \ldots, k)$ are the tap coefficients corresponding to the OD-ISI MR channel. n_i is the Gaussian noise with zero mean, variance $N_0/2$ and N_0 denotes the noise power-spectral density. In this paper, we primarily consider the extended class IV PR (EPR4) channel (i.e., $h_0 = 1, h_1 = 1, h_2 = -1, h_3 = -1$), which is commonly used in OD-ISI MR systems research.

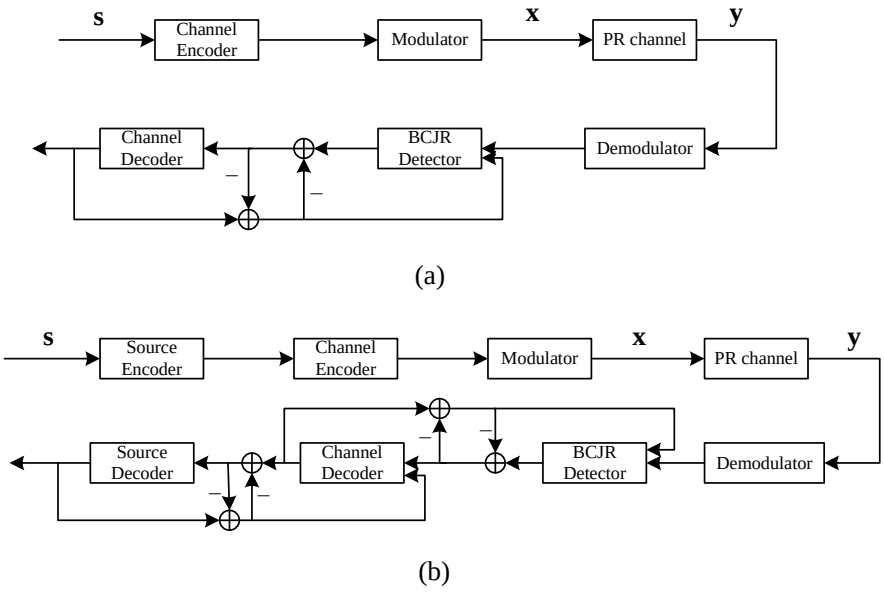

Figure 1. Block diagram of (**a**) the traditional separate channel coding system, (**b**) the proposed system over OD-ISI MR channels.

At the receiver, the decoder structure is processed iteratively by a three-stage serially concatenated framework, which contains a BCJR detector, a channel decoder and a source decoder. Different from the traditional Turbo equalization in Figure 1a, the residual redundancy left by source coding can be exploited by the three-stage serially concatenated Turbo equalization to further resist the ISI and improve the error performance of the system. As shown in Figure 1b, firstly, the BCJR detector uses its a priori information input to provide extrinsic information, which is passed to the channel decoder as a priori information. Secondly, the extrinsic information is exchanged between the channel decoder and the source decoder, which consists the JSCD iteration. After the JSCD iteration, finally, the output extrinsic information of the channel decoder is passed back to the BCJR detector as a priori information for further Turbo equalization iterations. Unlike the conventional Turbo equalization, in each Turbo equalization iteration of this system, the extrinsic infor-

mation is exchanged not only between the BCJR detector and the channel decoder, but also between the channel decoder and the source decoder. Here, the BCJR detector and the decoders are implemented by the BCJR algorithm and the belief propagation (BP) algorithm, respectively.

3. Convergence-Performance Analysis and Re-Design of PLDPC Channel Codes

3.1. M-JPEXIT Algorithm

Aiming to facilitate the asymptotic-performance analysis for the proposed system, the M-JPEXIT algorithm is provided in this subsection. Specifically, the M-JPEXIT algorithm is employed to investigate the MI evolution among the BCJR detector, the channel decoder, the source decoder and thus can be used to calculate the decoding thresholds of this system. In particular, the threshold value is assumed to be the minimum signal-to-noise ratio (SNR) per source bit (i.e., E_s/N_0) that allows to achieve error-free transmission.

To show the differences between the conventional JPEXIT algorithm and the proposed M-JPEXIT algorithm, the Tanner graphs of two algorithms are given in Figure 2. In Figure 2a, it is found that the initial log-likelihood ratios (LLRs) of the channel decoder in the JPEXIT algorithm can be derived from the output extrinsic LLRs of the AWGN channel. However, in M-JPEXIT algorithm, they are calculated by the LLR processor of the BCJR detector, which is shown Figure 2b. Furthermore, other than examining the evolution of the MIs exchanging between the channel decoder and the source decoder, the MIs exchanging between the channel decoder and the BCJR detector are taken into account in M-JPEXIT algorithm. Specifically, in Figure 2b, $\mathbf{B}_c$ with size of $m_c \times n_c$ and $\mathbf{B}_s$ with size of $m_s \times n_s$ represent the base matrices of the channel PLDPC code and the source PLDPC code, respectively. In addition, the (i,j)-th element of $\mathbf{B}_c(\mathbf{B}_s)$, denoted by $b_c^{i,j}$ ($b_s^{i,j}$), represents the number of edges connecting the VN v_j to the CN c_i in $\mathbf{B}_c(\mathbf{B}_s)$. The black squares represent the CNs of $\mathbf{B}_s$ and $\mathbf{B}_c$. The black circles in $\mathbf{B}_c$ indicate the source VNs for source coding and the black circles in $\mathbf{B}_s$ indicate the transmitted channel VNs for channel coding. In particular, the punctured channel VNs are denoted by empty circles. For the BCJR detector, the gray circles are used to represent the OD-ISI MR channel outputs and the squares denoted as trellis nodes are used to represent the state structure of the BCJR detector.

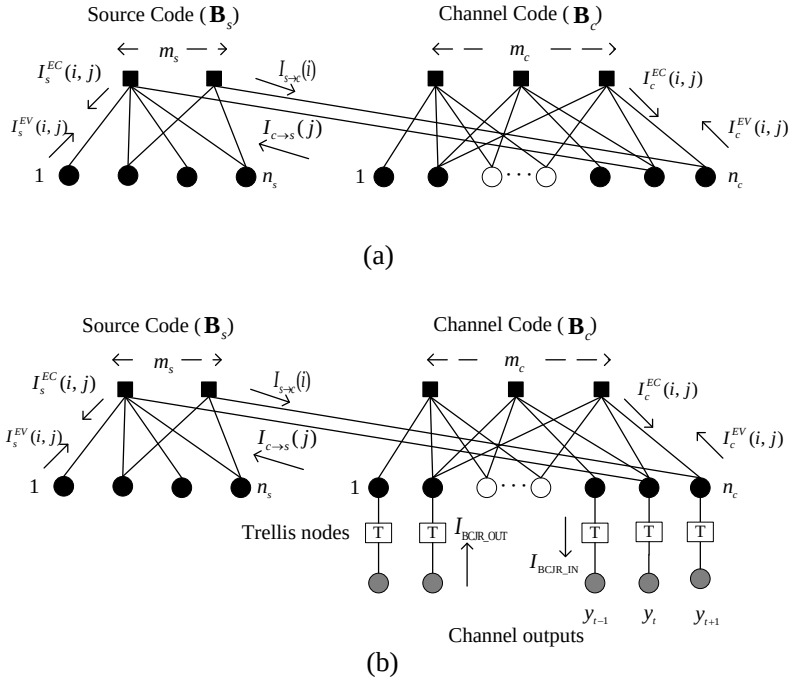

Figure 2. The Tanner graph of (**a**) the conventional JPEXIT algorithm, (**b**) the M-JPEXIT algorithm with MIs updating.

For the sake of introducing the M-JPEXIT algorithm in detail, nine types of MI are defined by:

(1) $I_{\text{BCJR\_OUT}}$: the extrinsic MI from the BCJR detector to VNs in $\mathbf{B}_c$.
(2) $I_{\text{BCJR\_IN}}$: the a prior MI from VNs in $\mathbf{B}_c$ to the BCJR detector.
(3) $I_{\text{s(c)}}^{\text{Ev}}(i,j)$: the extrinsic MI from the j-th VN to the i-th CN in $\mathbf{B}_{s(c)}$.
(4) $I_{\text{s(c)}}^{\text{Av}}(i,j)$: the a prior MI from the i-th CN to the j-th VN in $\mathbf{B}_{s(c)}$.
(5) $I_{\text{s(c)}}^{\text{Ec}}(i,j)$: the extrinsic MI from the i-th CN to the j-th VN in $\mathbf{B}_{s(c)}$.
(6) $I_{\text{s(c)}}^{\text{Ac}}(i,j)$: the a prior MI from the j-th VN to the i-th CN in $\mathbf{B}_{s(c)}$.
(7) $I_{\text{c}\to\text{s}}(j)$: the extrinsic MI from the j-th VN in $\mathbf{B}_c$ to the connected CN in $\mathbf{B}_s$.
(8) $I_{\text{s}\to\text{c}}(i)$: the extrinsic MI from the i-th CN in $\mathbf{B}_s$ to the connected VN in $\mathbf{B}_c$.
(9) $I_{\text{s}}^{\text{APP}}(j)$: the MI between the a posteriori LLR evaluated at j-th VN in $\mathbf{B}_s$ and the corresponding source bit.

$$\sigma_{\text{c}}^{\text{Ev\_1}} = \sqrt{\sum_{k\neq i} b_c^{k,j}[J^{-1}(I_c^{\text{Av}}(k,j))]^2 + \left(b_c^{i,j}-1\right)[J^{-1}(I_c^{\text{Av}}(i,j))]^2 + \left[J^{-1}\left(I_{\text{BCJR\_OUT}}\right)\right]^2}. \quad (3)$$

$$\sigma_{\text{c}}^{\text{Ev\_2}} = \sqrt{\sum_{k\neq i} b_c^{k,j}[J^{-1}(I_c^{\text{Av}}(k,j))]^2 + \left(b_c^{i,j}-1\right)[J^{-1}(I_c^{\text{Av}}(i,j))]^2 + \left[J^{-1}\left(I_{\text{BCJR\_OUT}}\right)\right]^2 + [J^{-1}(I_{s\to c}(j-(n_c-m_s)))]^2}. \quad (4)$$

$$\sigma_{\text{c}}^{\text{Ec}} = \sqrt{\sum_{k\neq j} b_c^{i,k}\left[J^{-1}\left(1-I_c^{\text{Ac}}(i,k)\right)\right]^2 + \left(b_c^{i,j}-1\right)\left[J^{-1}\left(1-I_c^{\text{Ac}}(i,j)\right)\right]^2}. \quad (5)$$

$$\sigma_{\text{BCJR\_IN}} = \sqrt{\sum_{k} b_c^{k,j}[J^{-1}(I_c^{\text{Av}}(k,j))]^2}. \quad (6)$$

$$\sigma_{\text{c}\to\text{s}} = \sqrt{\sum_{k} b_c^{k,j}[J^{-1}(I_c^{\text{Av}}(k,j))]^2 + \left[J^{-1}\left(I_{\text{BCJR\_OUT}}\right)\right]^2}. \quad (7)$$

$$\mu_{\text{s}}^{\text{Ev}} = \frac{1}{2}\sum_{k\neq i} b_s^{k,j}\left[J^{-1}\left(I_s^{\text{Av}}(k,j)\right)\right]^2 + \frac{1}{2}\left(b_s^{i,j}-1\right)\left[J^{-1}\left(I_s^{\text{Av}}(i,j)\right)\right]^2. \quad (8)$$

$$\sigma_{\text{s}}^{\text{Ec}} = \sqrt{\sum_{k\neq j} b_s^{i,k}\left[J^{-1}\left(1-I_s^{\text{Ac}}(i,k)\right)\right]^2 + \left(b_s^{i,j}-1\right)\left[J^{-1}\left(1-I_s^{\text{Ac}}(i,j)\right)\right]^2 + [J^{-1}(1-I_{c\to s}(i+n_c-m_s))]^2}. \quad (9)$$

$$\sigma_{s\to c} = \sqrt{\sum_{k} b_s^{i,k}\left[J^{-1}\left(1-I_s^{\text{Ac}}(i,k)\right)\right]^2}. \quad (10)$$

$$\mu_{\text{s}}^{\text{APP}} = \frac{1}{2}\sum_{k} b_s^{k,j}\left[J^{-1}\left(I_s^{\text{Av}}(k,j)\right)\right]^2. \quad (11)$$

The M-JPEXIT algorithm for the proposed system is detailed in Algorithm 1.

The iterative MI function $J(\cdot)$ of the channel decoder of Algorithm 1 is defined as

$$J(\sigma_{\text{ch}}) = 1 - \int_{-\infty}^{\infty} \frac{e^{-(\xi-\sigma_{\text{ch}}^2/2)^2/2\sigma_{\text{ch}}^2}}{\sqrt{2\pi\sigma_{\text{ch}}^2}} \log_2\left[1+e^{-\xi}\right] \mathrm{d}\xi, \quad (12)$$

where, $J(\sigma_{\text{ch}})$ represents the MI between a binary bit and channel LLR value $L_{\text{ch}} \sim N(\sigma_{\text{ch}}^2/2, \sigma_{\text{ch}}^2)$.

The inverse $J^{-1}(I)$ function is also given by

$$J^{-1}(I) = \begin{cases} a_1 I^2 + b_1 I + c_1 \sqrt{I}, & 0 \le I \le 0.3646, \\ -a_2 \ln[b_2(1-I)] - c_2 I, & 0.3646 < I < 1, \end{cases} \tag{13}$$

where, $a_1 = 1.09542, b_1 = 0.214217, c_1 = 2.33727, a_2 = 0.706692, b_2 = 0.386013$, $c_2 = -1.75017$.

The iterative MI function $J_{\mathrm{B}}(\cdot)$ of the source decoder of Algorithm 1 is

$$J_{\mathrm{B}}(\mu, p) = (1-p) \times I(V; \chi^{(1-p)}) + p \times I(V; \chi^{p}), \tag{14}$$

where, $I(V; \chi^{(1-p)}$ is the MI between the VN V of B_s and χ, μ represents the average LLR value obtained by V, $\chi^{(1-p)} \sim N(\mu + L_s, 2\mu)$, $\chi^{(p)} \sim N(\mu - L_s, 2\mu)$.

In Algorithm 1, the method to evaluate the MI $I_{\mathrm{BCJR\_OUT}}$ in line 9 is described as follows: for a given E_s/N_0, calculate the channel initial LLRs L_{ch} for the bit sequence output from the demodulator by Monte Carlo simulation and denote these LLR values as $\{L_{\mathrm{ch}}\}$. In addition, for a given a prior MI $I_{\mathrm{BCJR\_IN}}$ (set the initial $I_{\mathrm{BCJR\_IN}}$ as zero), the standard deviation $\sigma_{\mathrm{BCJR\_IN}}$ of the corresponding *a priori* LLRs $L_{\mathrm{BCJR\_IN}}$ can be calculated using (13) and generate the LLR sequence $\{L_{\mathrm{BCJR\_IN}}\}$ following the symmetric Gaussian distribution $N(\sigma^2_{\mathrm{BCJR\_IN}}/2, \sigma^2_{\mathrm{BCJR\_IN}})$. Passing the sequences $\{L_{\mathrm{ch}}\}$ and $\{L_{\mathrm{BCJR\_IN}}\}$ into the BCJR detector, we can measure the extrinsic LLR sequence of the BCJR detector $\{L_{\mathrm{BCJR\_OUT}}\}$ as (15). We then calculate the standard deviation $\sigma_{\mathrm{BCJR\_OUT}}$ of the sequence $\{L_{\mathrm{BCJR\_OUT}}\}$. Assuming that the sequence $\{L_{\mathrm{BCJR\_OUT}}\}$ follows a symmetric Gaussian distribution, we evaluate the MI $I_{\mathrm{BCJR\_OUT}}$ of the sequence $\{L_{\mathrm{BCJR\_OUT}}\}$ using (12).

$$L_{\mathrm{BCJR\_OUT}} = F(L_{\mathrm{ch}}, L_{\mathrm{BCJR\_IN}}), \tag{15}$$

where $F(\cdot)$ represents the LLR processor of the BCJR detector.

The threshold is the lowest value of E_s/N_0 ($(E_s/N_0)_{min}$) for which $I_{\mathrm{s}}^{\mathrm{APP}}(j) = 1$ for $j = 1 \cdots n_s$.

Note also that:

- The conventional JPEXIT algorithm tailored for JSCC systems is extended to a three-stage parallel concatenated system, which examines the evolution of the input/output MI exchanging among the BCJR detector, the channel decoder, and the source decoder.
- Different from the JPEXIT algorithm for AWGN channels, the modified algorithm is a hybrid performance analysis tool and it incorporates Monte Carlo simulation into information theoretical derivation.

3.2. A Re-Design Scheme for PLDPC Channel Codes

By taking advantage of the M-JPEXIT algorithm, a re-design method for channel codes of this system is provided in Algorithm 2. As is shown in [8], the edge connection between the VNs of the channel code and the CNs of the source code plays an important role in the error performance. Algorithm 2 also takes this edge connection into consideration.

Algorithm 1 M-JPEXIT algorithm for the proposed system.

Input: p, $\mathbf{B}_s$, $\mathbf{B}_c$, m_s, n_s, m_c, n_c;
the initial value of SNR x;
the number of Turbo equalization iteration N_t and the maximum number of JSC iteration N_j;
Start:
for $N_{t\_ini} = 1$ to N_t **do**
  for $j = 1$ to n_c **do**
    BCJR detector:
    Evaluate the MI $I_{\mathrm{BCJR\_OUT}}$;
  end for
  for $N_{j\_ini} = 1$ to N_j **do**
    Channel decoder:
    for $i = 1$ to m_c, $j = 1$ to n_c **do**
      Channel LLR initialization:
      The channel initial LLRs are defined by $\sigma_{\mathrm{BCJR\_OUT}}$. If v_j is punctured, $I_{\mathrm{BCJR\_OUT}} = 0$;
      The MI update between CNs and VNs:
      for $j = 1$ to $n_c - m_s$ **do**
        if $b_c^{i,j} = 0$ **then**
          $I_{\mathrm{c}}^{\mathrm{Ev}}(i,j) = 0$;
        else
          $I_{\mathrm{c}}^{\mathrm{Ev}}(i,j) = J(\sigma_{\mathrm{c}}^{\mathrm{Ev\_1}}) = I_{\mathrm{c}}^{\mathrm{Ac}}(i,j)$, $\sigma_{\mathrm{c}}^{\mathrm{Ev\_1}}$ is calculated as (3);
        end if
      end for
      for $j = n_c - m_s + 1$ to n_c **do**
        if $b_c^{i,j} = 0$ **then**
          $I_{\mathrm{c}}^{\mathrm{Ev}}(i,j) = 0$;
        else
          $I_{\mathrm{c}}^{\mathrm{Ev}}(i,j) = J(\sigma_{\mathrm{c}}^{\mathrm{Ev\_2}}) = I_{\mathrm{c}}^{\mathrm{Ac}}(i,j)$, $\sigma_{\mathrm{c}}^{\mathrm{Ev\_2}}$ is calculated as (4);
        end if
      end for
      if $b_c^{i,j} = 0$ **then**
        $I_{\mathrm{c}}^{\mathrm{Ec}}(i,j) = 0$;
      else
        $I_{\mathrm{c}}^{\mathrm{Ec}}(i,j) = 1 - J(\sigma_{\mathrm{c}}^{\mathrm{Ec}}) = I_{\mathrm{c}}^{\mathrm{Av}}(i,j)$, $\sigma_{\mathrm{c}}^{\mathrm{Ec}}$ is calculated as (5);
      end if
      The MI update from the channel decoder to the BCJR detector and the source decoder:
      $I_{\mathrm{BCJR\_IN}} = \frac{1}{n_c}\sum_{j=1}^{n_c} J(\sigma_{\mathrm{BCJR\_IN}})$, $\sigma_{\mathrm{BCJR\_IN}}$ is calculated as (6);
      $I_{\mathrm{c}\to\mathrm{s}}(j) = J(\sigma_{\mathrm{c}\to\mathrm{s}})$, $\sigma_{\mathrm{c}\to\mathrm{s}}$ is calculated as (7);
    end for
    Source decoder:
    for $i = 1$ to m_s, $j = 1$ to n_s **do**
      Source LLR initialization:
      $L_s = \ln((1-p)/p)$;
      The MI update between CNs and VNs:
      if $b_s^{i,j} = 0$ **then**
        $I_{\mathrm{s}}^{\mathrm{Ev}}(i,j) = 0$;
      else
        $I_s^{\mathrm{Ev}}(i,j) = J_B(\mu_{\mathrm{s}}^{\mathrm{Ev}}, p) = I_{\mathrm{s}}^{\mathrm{Ac}}(i,j)$, $\mu_{\mathrm{s}}^{\mathrm{Ev}}$ is calculated as (8);
      end if
      if $b_s^{i,j} = 0$ **then**
        $I_s^{\mathrm{Ec}}(i,j) = 0$;
      else
        $I_s^{\mathrm{Ec}}(i,j) = 1 - J(\sigma_{\mathrm{s}}^{\mathrm{Ec}}) = I_s^{\mathrm{Av}}(i,j)$, $\sigma_{\mathrm{s}}^{\mathrm{Ec}}$ is calculated as (9);
      end if
      The MI update from the source decoder to the channel decoder:
      $I_{s\to c}(i) = 1 - J(\sigma_{\mathrm{s}\to c})$, $\sigma_{\mathrm{s}\to c}$ is calculated as (10);
      A posteriori MI evaluation:
      $I_{\mathrm{s}}^{\mathrm{APP}}(j) = J_B(\mu_{\mathrm{s}}^{\mathrm{APP}}, p)$, $\mu_{\mathrm{s}}^{\mathrm{APP}}$ is calculated as (11);
    end for
    if $I_{\mathrm{s}}^{\mathrm{APP}}(1) = 1, \cdots, I_{\mathrm{s}}^{\mathrm{APP}}(n_s) = 1$ **then**
      goto Output;
    end if
  end for
end for
Set $x = x - 0.1$ and goto Start;
Output:
$(E_s/N_0)_{min} = x$.

Algorithm 2 Optimization algorithm for $\mathbf{B}_c$.

Require: p, $\mathbf{B}_s$, $\mathbf{B}_c$, m_s and n_c;
1: Calculate the system decoding threshold $Th(\mathbf{B}_c)$ by the proposed M-JPEXIT algorithm;
2: Generate initial: $\mathbf{B}_{c\_min} \leftarrow \mathbf{B}_c$, $Th(\mathbf{B}_{c\_min}) \leftarrow Th(\mathbf{B}_c)$;
3: Form $\mathbf{B}_{c\_en}$: Change the second largest degree VN of $\mathbf{B}_c$ into degree-1 VN and ensure the degree-1 VNs are connected to different CNs; Add the degrees of the VN with the largest degree of $\mathbf{B}_c$ to keep the degree of every CN unchanged;
4: **for** $i = 1$ to $\binom{n_c}{m_s}$ **do**
5: Select every m_s VNs of $\mathbf{B}_{c\_en}$ and connect them to the CVs of $\mathbf{B}_s$;
6: **for** $j = 1$ to n_c **do**
7: Puncture j-th VN of $\mathbf{B}_{c\_en}$ and Calculate $Th(\mathbf{B}_{c\_en})$;
8: **if** $Th(\mathbf{B}_{c\_en}) < Th(\mathbf{B}_{c\_min})$ **then**
9: $\mathbf{B}_{c\_min} \leftarrow \mathbf{B}_{c\_en}$, $Th(\mathbf{B}_{c\_min}) \leftarrow Th(\mathbf{B}_{c\_en})$;
10: **end if**
11: **end for**
12: **end for**
13: **return** $\mathbf{B}_{c\_min}$, $Th(\mathbf{B}_{c\_min})$.

Based on Algorithm 2, the best optimized channel code for PR channels in the separate coding system, which denoted as IARA2 in [22] is redesigned. The base matrix of $\mathbf{B}^{\mathrm{IARA2}}$ and its enhanced code $\mathbf{B}_{\mathrm{en}}^{\mathrm{IARA2}}$ are proposed in (16). Moreover, the optimized channel codes in JSCC systems over AWGN channels are utilized as benchmarks. For instance, the channel code in code pair $(\mathbf{B}^{\mathrm{s4}}, \mathbf{B}^{\mathrm{c2}})$ proposed in [9] and the channel code in code pair $\mathbf{B}_{\mathrm{J}}^{\mathrm{opti\_1}}$ proposed in [11] are redesigned by Algorithm 2. The base matrices ($\mathbf{B}^{\mathrm{c2}}$ and $\mathbf{B}_{\mathrm{c}}^{\mathrm{J}^{\mathrm{opti\_1}}}$) and the enhanced ones ($\mathbf{B}_{\mathrm{en}}^{\mathrm{c2}}$ and $\mathbf{B}_{\mathrm{en}}^{\mathrm{J}_{\mathrm{c}}^{\mathrm{opti\_1}}}$) are proposed in (17) and (18). For convenience of description, in all the base matrices below, the last two columns denote the VNs of channel codes connected to the source codes and the fourth column represents the punctured VN.

$$\mathbf{B}^{\mathrm{IARA2}} = \begin{pmatrix} 12100 \\ 01121 \\ 01211 \end{pmatrix} \quad \mathbf{B}_{\mathrm{en}}^{\mathrm{IARA2}} = \begin{pmatrix} 10021 \\ 01031 \\ 01112 \end{pmatrix} \tag{16}$$

$$\mathbf{B}^{\mathrm{c2}} = \begin{pmatrix} 10200 \\ 01111 \\ 01222 \end{pmatrix} \quad \mathbf{B}_{\mathrm{en}}^{\mathrm{c2}} = \begin{pmatrix} 10020 \\ 01111 \\ 01042 \end{pmatrix} \tag{17}$$

$$\mathbf{B}^{\mathrm{J}_{\mathrm{c}}^{\mathrm{opti\_1}}} = \begin{pmatrix} 12210 \\ 01111 \\ 00211 \end{pmatrix} \quad \mathbf{B}_{\mathrm{en}}^{\mathrm{J}_{\mathrm{c}}^{\mathrm{opti\_1}}} = \begin{pmatrix} 10104 \\ 01111 \\ 01102 \end{pmatrix} \tag{18}$$

4. Simulation Result and Discussion

To verify the merits of the enhanced channel codes, decoding thresholds and BER simulations of the JSCC systems over OD-ISI MR channels are presented in this section.

Table 1 provides the system decoding thresholds of the enhanced and the benchmark codes. In particular, for the IARA2 channel code in the separate coding system in [22], we employ 1/2-coderate R4JA code as the source code, and for the benchmark code pairs in JSCC systems, such as ($\mathbf{B}^{\mathrm{s4}}$, $\mathbf{B}^{\mathrm{c2}}$) in [9] and $\mathbf{B}_{\mathrm{J}}^{\mathrm{opti\_1}}$ in [11], the source codes in the original code pairs are reserved. As seen from Table 1, the system with enhanced channel codes possess lower decoding thresholds compared with the original counterparts.

Table 1. Decoding Thresholds of the Proposed System for Different Channel Codes and Source Statistics.

p	Channel Code	Threshold	Coding Gain
0.05	$\mathbf{B}^{\mathrm{IARA2}}/\mathbf{B}_{\mathrm{en}}^{\mathrm{IARA2}}$	$-3.1/-4.1$	1.0
	$\mathbf{B}^{\mathrm{c2}}/\mathbf{B}_{\mathrm{en}}^{\mathrm{c2}}$	$-3.3/-5.3$	2.0
	$\mathbf{B}^{\mathrm{J_c^{opti\_1}}}/\mathbf{B}_{\mathrm{en}}^{\mathrm{J_c^{opti\_1}}}$	$-3.4/-4.3$	0.9
0.06	$\mathbf{B}^{\mathrm{IARA2}}/\mathbf{B}_{\mathrm{en}}^{\mathrm{IARA2}}$	$-2.6/-3.3$	0.7
	$\mathbf{B}^{\mathrm{c2}}/\mathbf{B}_{\mathrm{en}}^{\mathrm{c2}}$	$-2.7/-4.3$	1.6
	$\mathbf{B}^{\mathrm{J_c^{opti\_1}}}/\mathbf{B}_{\mathrm{en}}^{\mathrm{J_c^{opti\_1}}}$	$-2.9/-3.6$	0.7

Figure 3 plots the BER curves of the proposed system with enhanced channel codes and original counterparts at $p = 0.05$. The number of Turbo equalization iteration is set to 5 and the maximum number of JSCD iteration is set to 100. The frame length is fixed at 3200 bits and the protograph is generated using the progressive edge growth (PEG) algorithm [29]. It is observed that at a BER of 10^{-5}, $\mathbf{B}_{\mathrm{en}}^{\mathrm{IARA2}}$ achieves coding gain of 0.5 dB over $\mathbf{B}^{\mathrm{IARA2}}$; $\mathbf{B}_{\mathrm{en}}^{\mathrm{c2}}$ and $\mathbf{B}_{\mathrm{en}}^{\mathrm{J_c^{opti\_1}}}$ have 0.5 dB and 0.6 dB gains compared with $\mathbf{B}^{\mathrm{c2}}$ and $\mathbf{B}^{\mathrm{J_c^{opti\_1}}}$, respectively, at a BER of 10^{-5}.

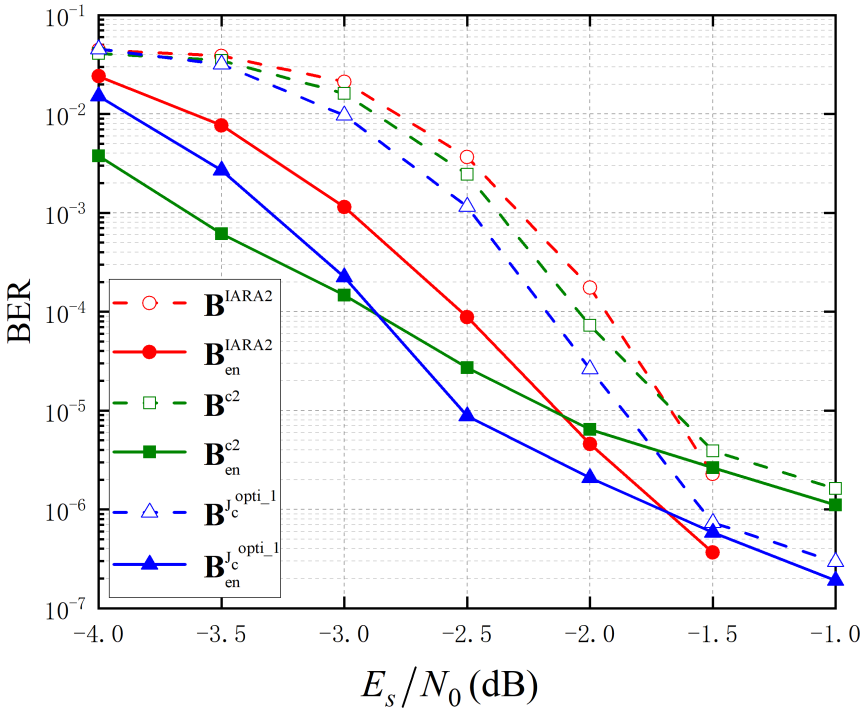

Figure 3. Simulated BER results of the enhanced and the benchmark codes at $p = 0.05$.

Figure 4 shows the BER performance with different channel codes at $p = 0.06$. It can be observed that the enhanced channel codes all have better error performance than the original counterparts in the water-fall region. Clearly, the superiorities of the enhanced channel codes over the benchmark codes in the BER performance are consistent with the analysis results of system decoding thresholds shown in Table 1.

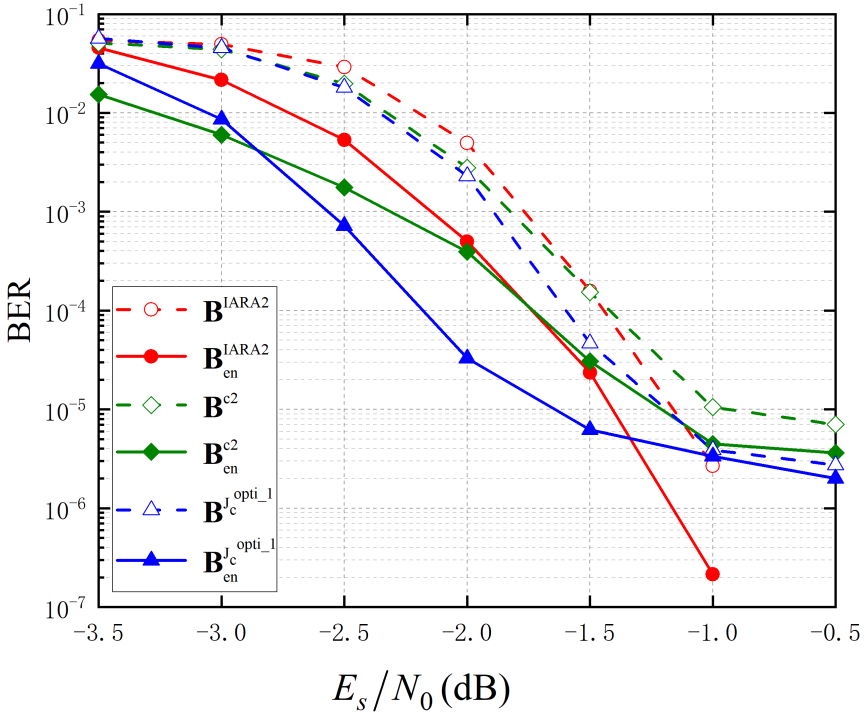

Figure 4. Simulated BER results of the enhanced and the benchmark codes at $p = 0.06$.

5. Conclusions

In this paper, firstly we combine the JSCC technique with Turbo equalization and investigate this system over OD-ISI MR channels. Moreover, by means of the M-JPEXIT algorithm, a re-design scheme for the channel codes in the proposed system is put forward to improve the error performance. Both the M-JPEXIT analysis and the BER simulation results show the performance improvement of the enhanced channel codes, especially in the water-fall region.

In future work, the optimization of the JSC decoder for the JSCC system over OD-ISI magnetic recording channels will be investigated.

Author Contributions: Conceptualization, C.C.; Data curation, Y.S.; Formal analysis, Q.C.; Funding acquisition, C.C. and Q.C.; Investigation, Y.S.; Methodology, C.C.; Project administration, C.C.; Resources, S.L.; Software, Y.S.; Supervision, C.C.; Validation, S.L.; Writing—original draft, Y.S.; Writing—review & editing, C.C. and L.Z. All authors have read and agreed to the published version of the manuscript.

Funding: This research received National Natural Science Foundation of China: 61901182; National Natural Science Foundation of China: 62101195; Science Foundation of the Fujian Province, China: 2020J05056; Scientific Research Funds of Huaqiao University under Grant: 19BS206; the Scientific Research Funds of Huaqiao University under Grant: 21BS118.

Data Availability Statement: Not applicable.

Conflicts of Interest: The authors declare no conflict of interest.

Abbreviations

The following abbreviations are used in this manuscript:

AWGN	Additive White Gaussian Noise
BER	Bit-Error-Rate
BPSK	Binary-Phase-Shift-keying
BCJR	Bahl–Cocke–Jelinek–Raviv
BP	Belief Propagation
CN	Check Node
DP-LDPC	Double Protograph Low-Density Parity-Check
ECC	Error Correction Code
EPR4	Extended Class IV PR
i.u.d	independent and uniformly distributed
ISI	Inter-Symbol-Interference
JSCC	Joint Source-Channel Coding
JSCD	Joint Source-Channel Decoder
LLR	Log-Likelihood Ratio
LDPC	Low-Density Parity-Check
M-JPEXIT	Modified Joint Protograph Extrinsic Information Transfer
MR	Magnetic Recording
MI	Mutual Information
OD-ISI	One-Dimensional Inter-Symbol-Interference
PLDPC	Protograph Low-Density Parity-Check
PR	Partial Response
PEG	Progressive Edge Growth
SNR	Signal-to-Noise Ratio
TD-ISI	Two-Dimensional Inter-Symbol-Interference
VN	Variable Node

References

1. Pu, L.; Wu, Z.; Bilgin, A.; Marcellin, M.W.; Vasic, B. LDPC-based iterative joint source-channel decoding for JPEG2000. *IEEE Trans. Image Process.* **2007**, *16*, 577–581. [CrossRef] [PubMed]
2. Zribi, A.; Pyndiah, R.; Zaibi, S.; Guilloud, F.; Bouallegue, A. Low-complexity soft decoding of Huffman codes and iterative joint source channel decoding. *IEEE Trans. Commun.* **2012**, *60*, 1669–1679. [CrossRef]
3. Gallager, R. Low-density parity-check codes. *IRE Trans. Inf. Theory* **1962**, *8*, 21–28. [CrossRef]
4. Fresia, M.; Perez-Cruz, F.; Poor, H.V.; Verdu, S. Joint source and channel coding. *IEEE Signal Process. Mag.* **2010**, *27*, 104–113. [CrossRef]
5. Thorpe, J.T. Low-density parity-check (LDPC) codes constructed from protographs. *IPN Progress Rep.* **2003**, *42*, 42–154.
6. He, J.; Wang, L.; Chen, P. A joint source and channel coding scheme base on simple protograph structured codes. In Proceedings of the 2012 International Symposium on Communications and Information Technologies (ISCIT), Gold Coast, QLD, Australia, 2–5 October 2012; pp. 65–69.
7. Chen, Q.; Wang, L.; Hong, S.; Xiong, Z. Performance improvement of JSCC scheme through redesigning channel code. *IEEE Commun. Lett.* **2016**, *20*, 1088–1091. [CrossRef]
8. Hong, S.; Chen, Q.; Wang, L. Performance analysis and optimisation for edge connection of JSCC system based on double protograph LDPC codes. *IET Commun.* **2018**, *12*, 214–219. [CrossRef]
9. Chen, C.; Wang, L.; Lau, F.C. Joint optimization of protograph LDPC code pair for joint source and channel coding. *IEEE Trans. Commun.* **2018**, *66*, 3255–3267. [CrossRef]
10. Chen, Q.; Wang, L.; Hong, S.; Chen, Y. Integrated design of JSCC scheme based on double protograph LDPC codes system. *IEEE Commun. Lett.* **2019**, *23*, 218–221. [CrossRef]
11. Liu, S.; Wang, L.; Chen, J.; Hong, S. Joint component design for the JSCC system based on DP-LDPC codes. *IEEE Trans. Commun.* **2020**, *68*, 5808–5818. [CrossRef]
12. Chen, Q.; Lau, F.C.; Wu, H.; Chen, C. Analysis and improvement of error-floor performance for JSCC scheme based on double protograph LDPC codes. *IEEE Trans. Veh. Technol.* **2020**, *69*, 14316–14329. [CrossRef]
13. Chen, C.; Chen, Q.; Wang, L.; He, Y.C.; Chen, Y. Probabilistic shaping for protograph ldpc-coded modulation by residual source redundancy. *IEEE Trans. Commun.* **2021**, *69*, 4267–4281. [CrossRef]
14. Xu, Z.; Wang, L.; Hong, S.; Chen, G. Design of code pair for protograph-ldpc codes-based jscc system with joint shuffled scheduling decoding algorithm. *IEEE Trans. Commun.* **2021**, *25*, 3770–3774. [CrossRef]

15. Douillard, C.; Jézéquel, M.; Berrou, C.; Electronique, D.; Picart, A.; Didier, P.; Glavieux, A. Iterative correction of intersymbol interference: turbo-equalization. *Eur. Trans. Telecommun.* **1995**, *6*, 507–511. [CrossRef]
16. Raphaeli, D.; Zarai, Y. Combined turbo equalization and turbo decoding. *IEEE Commun. Lett.* **1998**, *2*, 107–109. [CrossRef]
17. Kurkoski, B.M.; Siegel, P.H.; Wolf, J.K. Joint message-passing decoding of LDPC codes and partial-response channels. *IEEE Trans. Inf. Theory* **2002**, *48*, 1410–1422. [CrossRef]
18. Song, H.; Todd, R.M.; Cruz, J. Low density parity check codes for magnetic recording channels. *IEEE Trans. Magn.* **2000**, *36*, 2183–2186. [CrossRef]
19. Jiao, X.; Mu, J.; He, Y.C.; Xu, W. Linear-complexity ADMM updates for decoding LDPC Codes in partial response channels. *IEEE Commun. Lett.* **2019**, *23*, 2200–2204. [CrossRef]
20. Jiao, X.; Liu, H.; Mu, J.; He, Y.C. l_2-Box ADMM decoding for LDPC codes over ISI channels. *IEEE Trans. Veh. Technol.* **2021**, *70*, 3966–3971. [CrossRef]
21. Zhang, Y.; Wu, H.; Coates, M. On the design of channel coding autoencoders with arbitrary rates for ISI channels. *IEEE Wirel. Commun. Lett.* **2022**, *11*, 426–430. [CrossRef]
22. Fang, Y.; Chen, P.; Wang, L.; Lau, F.C. Design of protograph LDPC codes for partial response channels. *IEEE Trans. Commun.* **2012**, *60*, 2809–2819. [CrossRef]
23. Yang, S.; Wang, L.; Fang, Y.; Chen, P. Performance of improved AR3A code over EPR4 channel. In Proceedings of the the 2011 3rd International Conference on Computer Research and Development, Shanghai, China, 11–13 March 2011; pp. 60–64.
24. Van Nguyen, T.; Nosratinia, A.; Divsalar, D. Protograph-based LDPC codes for partial response channels. In Proceedings of the 2012 IEEE International Conference on Communications (ICC), Ottawa, ON, Canada, 10–15 June 2012; pp. 2166–2170.
25. Van Nguyen, T.; Nosratinia, A.; Divsalar, D. Rate-compatible protograph-based LDPC codes for inter-symbol interference channels. *IEEE Commun. Lett.* **2013**, *17*, 1632–1635. [CrossRef]
26. Chen, P.; Kong, L.; Fang, Y.; Wang, L. The design of protograph LDPC codes for 2-D magnetic recording channels. *IEEE Trans. Magn.* **2015**, *51*, 1–4. [CrossRef]
27. Chen, P.; Kui, C.; Kong, L.; Chen, Z.; Zhang, M. Non-binary protograph-based LDPC codes for 2-D-ISI magnetic recording channels. *IEEE Trans. Magn.* **2017**, *53*, 1–5.
28. Fang, Y.; Han, G.; Cai, G.; Lau, F.C.; Chen, P.; Guan, Y.L. Design guidelines of low-density parity-check codes for magnetic recording systems. *IEEE Commun. Surv. Tuts.* **2018**, *20*, 1574–1606. [CrossRef]
29. Hu, X.Y.; Eleftheriou, E.; Arnold, D.M. Regular and irregular progressive edge-growth tanner graphs. *IEEE Trans. Inf. Theory* **2005**, *51*, 386–398. [CrossRef]